

Accepted Manuscript

Why are maternally separated females inflexible? Brain activity pattern of COx and c-Fos

María Banqueri, Marta Méndez, Jorge L. Arias

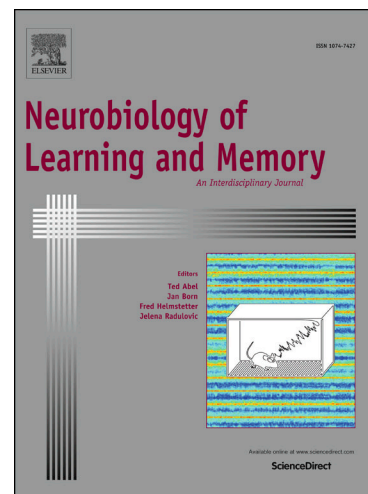
PII: S1074-7427(18)30144-8
DOI: <https://doi.org/10.1016/j.nlm.2018.06.007>
Reference: YNLME 6888

To appear in: *Neurobiology of Learning and Memory*

Received Date: 4 December 2017
Revised Date: 6 June 2018
Accepted Date: 13 June 2018

Please cite this article as: Banqueri, M., Méndez, M., Arias, J.L., Why are maternally separated females inflexible? Brain activity pattern of COx and c-Fos, *Neurobiology of Learning and Memory* (2018), doi: <https://doi.org/10.1016/j.nlm.2018.06.007>

This is a PDF file of an unedited manuscript that has been accepted for publication. As a service to our customers we are providing this early version of the manuscript. The manuscript will undergo copyediting, typesetting, and review of the resulting proof before it is published in its final form. Please note that during the production process errors may be discovered which could affect the content, and all legal disclaimers that apply to the journal pertain.



Why are maternally separated females inflexible? Brain activity pattern of COx and c-Fos

María Banqueri^{ab*}, Marta Méndez^{ab}, Jorge L. Arias^{ab}

^a Laboratory of Neuroscience, Department of Psychology. University of Oviedo, Plaza Feijoo, s/n, E-33003, Oviedo, Spain.

^bInstituto de Neurociencias del Principado de Asturias (INEUROPA)

*Corresponding author: Department of Psychology. University of Oviedo, Plaza Feijoo, s/n, E-33003, Oviedo, Spain. E-mail address: uo247593@uniovi.es (M. Banqueri) Phone Number: +34 985 10 32 12

Abstract

Subjects' early life events will affect them later in life. When these events are stressful, such as child abuse in humans or repeated maternal separation in rodents, subjects can show some behavioral and brain alterations. This study used young adult female Wistar rats that were maternally raised (AFR), maternally separated from post-natal day (PND) 1 to PND10 (MS10), or maternally separated from PND1 to PND21 (MS21), in order to assess the effects of maternal separation (MS) on spatial learning and memory, as well as cognitive flexibility, using the Morris Water Maze (MWM). We performed quantitative cytochrome oxidase (COx) histochemistry on selected brain areas in order to identify whether maternal separation affects brain energy metabolism. We also performed c-Fos immunohistochemistry on the medial prefrontal cortex (mPFC), thalamus, and hippocampus to explore whether this immediate early gene activity was altered in stressed subjects. We obtained a similar spatial learning pattern in maternally raised and maternally separated subjects on the reference memory task, but only the controls were flexible enough to solve the reversal learning successfully. Separated groups showed less c-Fos activity in the mPFC and less complex neural networks on COx.

Key Words:

Females

Early life stress

Reference memory

Flexibility

Cytochrome Oxidase

c-Fos

1 Introduction

Early life stress leads to cognitive impairments in adulthood (Cabeza de Baca & Ellis, 2017; Lejeune et al., 2013). Dam-litter interaction is essential for the optimal neurodevelopment of the offspring. Dams provide pups with maternal care, including grooming, licking, feeding and general nursing. Hence, commonly used early life stress models demonstrate the disruption of this relationship. However, comparing results from different laboratories is sometimes problematic due to variability in experimental designs. For instance, some research groups prefer maternal deprivation (MD), which involves separating the dam from the litter on postnatal day 9 (PND9) for 24 hours (Marković et al., 2014), whereas others prefer to separate repeatedly (i.e. 4 h/day PND 1-21 (Wang, Li, Du, Shao, & Wang, 2015) or for ten days (Felice et al., 2014). Due to this variability, our aim was to compare these different models.

The spatial orientation network includes the extended hippocampal system proposed by the Aggleton research group (Jankowski et al., 2013), including the hippocampus itself and its cortices, anterior thalamus, mammillary bodies, ventral tegmental area, amygdala, and medial prefrontal cortex (mPFC) (Aggleton, 2012). Retrosplenial areas are also related to spatial memory tasks (Jenkins, Amin, Harold, Pearce, & Aggleton, 2003). Thus, we aimed to study all of these areas.

In this study, we used two lengths of early maternal separation (MS) and tested the subjects on reference memory and reversal learning in the Morris Water Maze (MWM) to explore spatial memory and cognitive flexibility. We also investigated whether the brain substrates, using two different techniques: quantitative cytochrome oxidase (COx) histochemistry (Gonzalez-Lima & Cada, 1994) and c-Fos immunohistochemistry (Méndez-López, Méndez, López, & Arias, 2009), were different in stressed and non-stressed animals. First, we used the COx technique to address the amount of brain

energy metabolism used to solve the tasks. Second, the c-Fos immunohistochemistry technique allowed us to determine quantities of c-Fos-encoded protein. c-Fos encoded protein is the product of the c-Fos oncogene, which is useful for providing information about the neuronal activity required for spatial memory processes (Méndez-López, Méndez, López, & Arias, 2009).

Numerous studies have investigated the effects of early-life stress, but only in the past decade have females been included in the research cohorts (Barbosa Neto et al., 2012; Dalaveri, Nakhaee, Esmailpour, Mahani, & Sheibani, 2017; Dimatelis, Vermeulen, Bugarith, Stein, & Russell, 2016; Loi et al., 2015; Lukkes, Meda, Thompson, Freund, & Andersen, 2017; Majcher-maslanka, Solarz, Krzysztof, & Chocyk, 2017; Sun, Tu, Shi, Xue, & Zhao, 2014; Xiong, Yang, Wang, Xu, & Mao, 2014). In a previous study in our laboratory, we demonstrated how MS affects male rats' spatial memory (Banqueri, Méndez, & Arias, 2017). In the present study, we want to further explore spatial memory, in this case with females, while also testing cognitive flexibility. Thus, the novelties of these experiments are the exploration of females, which are sometimes not intensively explored, the addition of cognitive flexibility testing, rather than spatial memory alone, and the comparison of two neural activity techniques: c-Fos and COx.

2 Materials and Methods

2.1 Animals

Thirty newborn female Wistar rats were taken from the animalarium at Oviedo University. All the animals received ad libitum food and tap water and were maintained at a constant room temperature (22 ± 2 °C), with a relative humidity of 65-75% and an artificial light-dark cycle of 12h (08:00-20:00/20:00-08:00). The procedures and manipulation of the animals used in this study were carried out according to the Directive (2010/63/EU), Royal Decree 53/2013 of the Ministry of the Presidency,

related to the protection of animals used for experimentation and other scientific purposes, and they were approved by the Principality of Asturias committee for animal studies.

2.2 Maternal separation

Litters were randomly assigned to maternal separation or animal facility rearing (AFR) conditions. Litters with more than 10 animals were culled to 10, with approximately the same number of males and females in each. For MS, litters were separated from the dams for 4 hours per day, starting at 10:00 hours and ending at 14:00 hours. The MS21 group was separated from PND 1 to PND 21, whereas the MS10 group was separated from PND 1 to PND 10.

Each separation consisted of removing the dams from the home cage and placing them in an adjacent cage while the pups were kept together in a new cage. Litters remained together during the separation time in an incubator (30 °C, 55-65% relative humidity). After the separation period, the dam and the litter were returned to the home cage (placing the litter in the home cage first). Control litters were reared under standard animal facility rearing (AFR) conditions, disturbed only by animal facility husbandry practices once a week until weaning. On PND 21, all the animals were weaned and segregated by sex, and only females were selected for the study.

Therefore, three groups of female animals were included in the experiment, one control group, or AFR (n = 10), and two experimental groups: MS10 (n = 10) and MS21 (n = 10).

Figure 1- Experimental Timeline

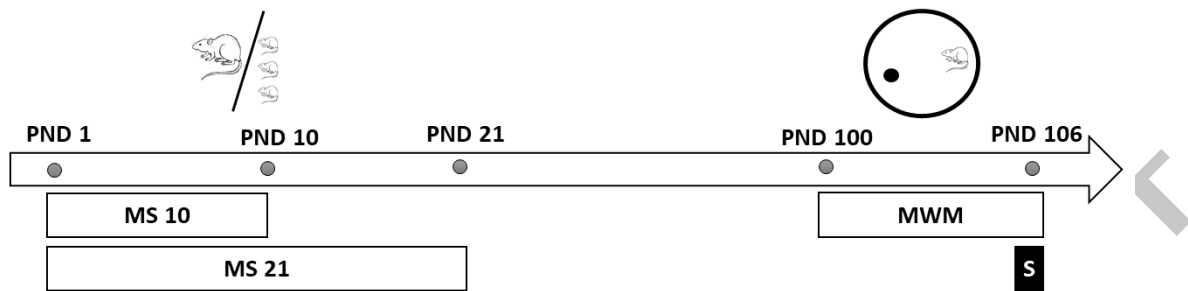


Figure 1: From PND 1 to PND 10, the MS10 animals were separated from their dams (10 MS10 females). From PND 1 to PND 21 (n=10), the MS21 animals were separated from their dams (10 MS21 females) (n=10). PND = Post-natal day, MS = Maternal separation, MWM= Morris Water Maze, S= Sacrifice

2.3 Vaginal smears

Six rats per group were randomly chosen for this procedure. Vaginal smears were taken from females on four consecutive days at approximately PND60 to determine the different stages of the estrous cycle. In order to determine the different stages of the estrous cycle, we use the direct cytology method (Marcondes, Binchi, & Tanno, 2002). This method consists of exposing 0.9 NaCl in the rat's vagina with a pipette, and then absorbing the liquid. The liquid is mounted on a slide and observed with a light microscope (Leica DFC490, Germany). Cellular type, number, and disposition criteria were used to determine the stage of the estrous cycle. All the rats showed normal estrous cycles.

2.4 Morris Water Maze task

On PND 100, the animals' behavior was tested in the Morris water maze (MWM), as previously described (Méndez-López, Méndez, López, & Arias, 2009). The apparatus consisted of a black cylindrical fiberglass tank measuring 150 cm in diameter by 75 cm in height, placed 35 cm above the floor. Water level was 30 cm, at a temperature of 22 ± 2 °C. The escape platform used was a cylinder measuring 10 cm in diameter and 28 cm in height, placed 2 cm below the surface of the water. The MWM was located in

the center of a 16 m² lit room (two lamps of 4000 lx oriented towards the walls), surrounded by black panels (30 cm from the maze) on which the spatial cues were placed (horizontal line, vertical line, and a square rotated 45°, all yellow or black and yellow). The pool was divided into four imaginary quadrants (A, B, C and D) to locate start positions and platforms. The animal's behavior was recorded, and its path was analyzed using a computerized video-tracking system (Ethovision Pro, Noldus Information Technologies, Wageningen, The Netherlands).

In the learning protocol, the first day was devoted to the animals' habituation to the task. Thus, the animals performed four trials with a visible platform that protruded 4 cm from the water and was located in the center of the pool. On the following four days, the animals were required to locate a hidden platform located in the center of quadrant D in relation to the external visual cues on training days. Training took place in a block of four trials per day. To begin each trial, the rats were placed in the water, facing the maze wall in one of four quadrants, and the daily order of entry into these quadrants was pseudo-randomized. Each trial ended once the animal had found the hidden platform, or when 60 s had elapsed. If the animal had not reached the hidden platform after this time, it was placed on the platform for 15 s. During the inter-trial interval, the animals were placed in a black bucket for 30 s. The time and distance swum in each trial were recorded. At the end of the session, a probe test was applied where the pool platform was removed and the rat was introduced into the pool for 25 s in the quadrant opposite to where the platform had been located in previous trials, in order to find out whether the animal remembered the position of the platform. Immediately after the probe test, the animals were subjected to an additional trial with the hidden platform placed in its usual position to avoid any possible interference with the probe test. Latencies were recorded during acquisition, as well as the time of permanence in each quadrant during the probe test.

After this training, the rats were tested on reversal learning for one day using the previously described procedure (Arias, Fidalgo, Méndez, & Arias, 2015). The animals were given eight acquisition trials where the hidden platform was located in the quadrant opposite its previous location, quadrant C. As in the memory training, the rats were given a 25-second probe test at the end of the session (See Figure 2).

Figure 2- Morris Water Maze procedure

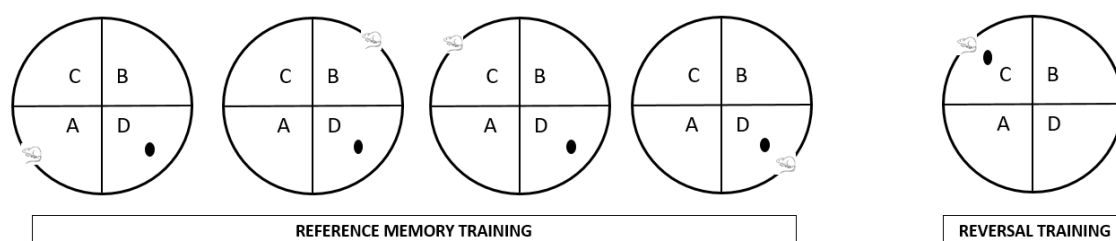


Figure 2 shows a schematic view of the MWM. In Reference memory training (left), you can see an example of the first four trials on one day of reference memory training. The animal is released from every quadrant, and the platform remains in the same place. In reversal training (right), an example trial is shown, where the platform has changed its initial position, and the animal is released from a different quadrant.

2.5 c-Fos Immunocytochemistry

Ninety minutes after the behavioral task in the MWM ended, the animals were decapitated. Brains were removed, frozen rapidly in N-methyl butane (Sigma-Aldrich, Madrid, Spain), and stored at -40°C until processing with c-Fos immunocytochemistry for frozen tissue (Arias, Méndez, & Arias, 2015). Coronal sections ($30\ \mu\text{m}$) of the brain were cut at -22°C in a cryostat (Leica CM1900, Germany) and mounted on gelatinized slides. The sections were post-fixed in buffered 4% paraformaldehyde (0.1M, pH7.4) for 30 min and rinsed in phosphate-buffered saline (PBS) (0.01 M, pH 7.4). They were subsequently incubated for 15 min with 3% hydrogen peroxidase in PBS to remove endogenous peroxidase activity, and then washed twice in PBS. After blocking with a PBS solution containing 10% Triton X-100 (PBS-T) (Sigma, USA) and 3% bovine

serum albumin for 30 min, sections were incubated with a rabbit polyclonal anti-c-Fos solution (1:10,000) (Santa Cruz Biotech, sc-52, USA) diluted in PBS-T for 24 h at 4 °C in a humid chamber. Slides were then washed 3 times with PBS and incubated in a goat anti-rabbit biotinylated IgG secondary antibody (Pierce, USA; diluted 1:200 in incubating solution) for 2 h at room temperature. They were washed 3 times in PBS and reacted with avidin–biotin peroxidase complex (Vectastain ABC Ultrasensitive Elite Kit, Pierce) for 1 h. After 2 washes in PBS, the reaction was visualized by treating the sections for approximately 3 min in a commercial nickel-cobalt-intensified diaminobenzidine kit (Pierce). The reaction was finalized by washing the sections twice in PBS. Slides were then dehydrated through a series of graded alcohols, cleared with xylene, and cover-slipped with Entellan (Merck, USA) for microscopic observation. All immunocytochemistry procedures included sections that served as controls, where the primary antibody was not added. Slides containing sections of a specific brain region were stained at the same time. Slides were coded so that the investigator who performed the analysis would be blind to the treatment of the individual subjects.

2.6 Cytochrome oxidase histochemistry

Ninety minutes after the behavioral task in the MWM ended, the animals were decapitated. Brains were removed, frozen rapidly in N-methyl butane (Sigma-Aldrich, Madrid, Spain), and stored at -40 °C until processing with quantitative COx histochemistry, as described by González-Lima and Cada (Gonzalez-Lima & Cada, 1994). Coronal sections (30 µm) of the brain were cut at -22 °C in a cryostat (Leica CM1900, Germany) and mounted on non-gelatinized slides. To quantify enzymatic activity and control staining variability across different baths, sets of tissue homogenate standards from the Wistar rats' brains (12 brains were used to create tissue homogenate, and they were treated in the same way as experimental brains) (Poremba, Jones, & Gonzalez-Lima, 1998) were cut at different thicknesses (10, 30, 50 and 70 µm). These tissues were included with each bath of slides to generate a

single regression equation between CO activity and the optical density of the sections for the subsequent comparison of all the tissues in the present experiment. The sections and standards were incubated for 5 minutes in 0.1 phosphate buffer with 10% (w/v) sucrose and 0.5 (v/v) glutaraldehyde, pH 7.6. Next, baths of 0.1M phosphate buffer with 10% (w/v) sucrose were given for 5 minutes each. Subsequently, 0.05M Tris buffer, pH7.6, with 275 mg/l cobalt chloride, 10% w/v sucrose, and 0.5 (v/v) dimethyl-sulfoxide, was applied for 10 min. Then, sections and standards were incubated in a solution of 0.06g cytochrome c, 0.016g catalase, 40g sucrose, 2 ml dimethyl-sulfoxide, and 0.4g diaminobenzidine tetra-hydrochloride (Sigma-Aldrich, Madrid, Spain) in 800ml of 0.1M phosphate buffer at 37°C for 1h. The reaction was stopped by fixing the tissue in buffered formalin for 30 minutes at room temperature with 10% (w/v) sucrose and 4% (v/v) formalin. Finally, the slides were dehydrated, cleared with xylene, and cover-slipped with Entellan (Merck, Germany).

2.7 c-Fos positive cell counting

The total number of c-Fos positive nuclei was quantified in six alternate sections 30 μm apart (with a section between them, used for COx staining) containing the IL, PL, and CG cortex, thalamic nuclei (Anteroventral, AV; anteromedial, AM), and dorsal hippocampus (CA1, DG). Coronal sections of these brain regions were located using the stereotaxic atlas by Paxinos and Watson (Paxinos & Watson, 2005). Distance of brain regions in mm counted from bregma was: +3.2 for IL, PL and CG cortex, -1.72 for thalamic nuclei, and -3.24 for dorsal hippocampus. Quantification was done by systematically sampling each of the regions selected using counting frames superimposed over the region (42025 μm^2 for the thalamus and medial prefrontal cortex and 160000 μm^2 for the hippocampus). Cell counts were conducted using a microscope (Leica DFC490, Germany) coupled to a computer with certain software installed (Leica application suite, Germany). c-Fos positive nuclei were defined based on homogenous gray-black stained elements with a well-defined border. Finally, the

mean count of six sections (12 counting frames per area, 6 animals per group) was calculated for each subject and region.

2.8 COx optical density quantification

The COx histochemical staining intensity was quantified by means of densitometric analysis, using a computer-assisted image analysis workstation (MCID, Interfocus ImagingLtd., Linton, England) composed of a high precision illuminator, a digital camera, and a computer with specific image analysis software. The mean optical density (OD) of each region was measured on bilateral structures using three consecutive sections in each subject (n=10 subjects per group). In each section, four non-overlapping readings were taken, using a square-shaped sampling window adjusted for each region size (See Figure 3). A total of twelve measurements were taken per region by an investigator who was blind to the groups. These measurements were averaged to obtain one mean per region for each animal. OD values were then converted to COx activity units, determined by the enzymatic activity of the standards measured spectrophotometrically (Gonzalez-Lima & Cada, 1994). The regions of interest were anatomically defined according to Paxinos and Watson's atlas (Paxinos & Watson, 2005). The regions of interest and the distance in mm of the regions counted from bregma were: +3.20mm for the infralimbic (IL),prelimbic (PL), and Cingulate (CG) cortices; +0.24 mm for the accumbens core (AcC) accumbens shell (AcSh), and dorsal striatum (ST); -1.20 mm for the CA1, CA3, and dentate gyrus (DG) subfields of the dorsal HC;-2.04 for the retrosplenial agranular (RSA) and retrosplenial granular (RSG) cortices and the thalamus anterodorsal, anteroventral and anteromedial (AD, AV, AM); -4.56 mm for the supramammilar (SuM), Medial medial mamilar (MMM), Medial lateral mamilar (MML), and ventral tegmental area (VTA); and -5.04mm for the entorhinal (ENT) and perirhinal cortices (PRh).

Figure 3- Regions of Interest

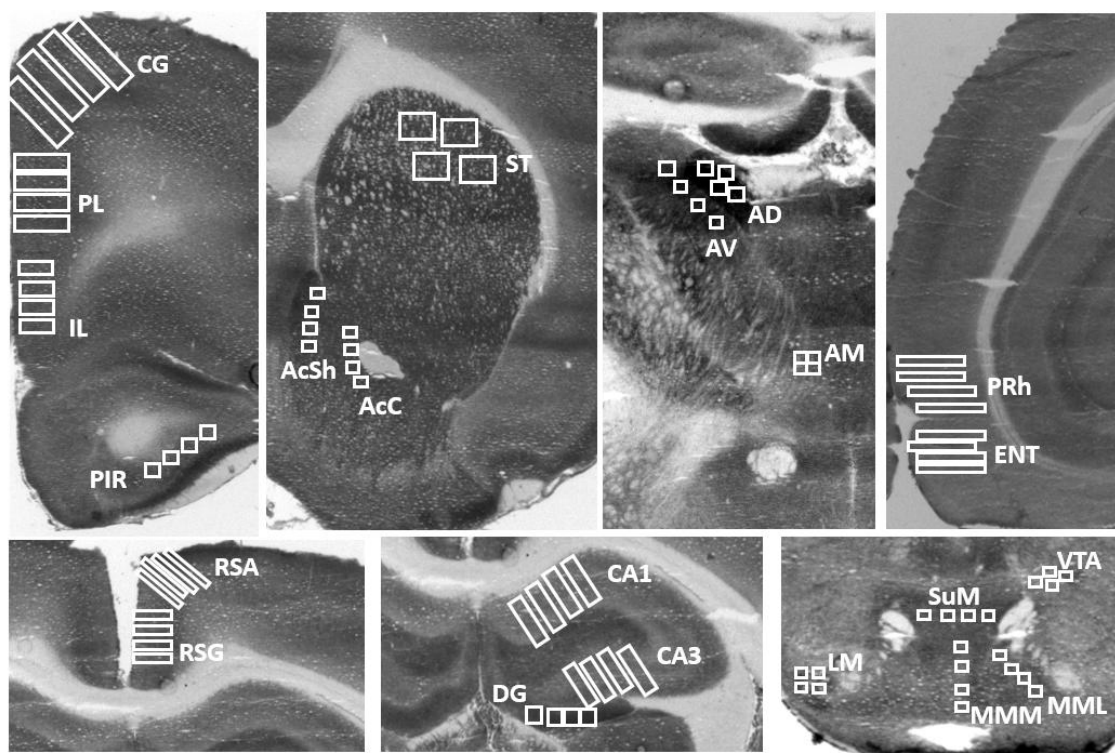


Figure 3. Sampling frames of COx histochemistry in the regions of interest. Infralimbic cortex= IL, Prelimbic cortex=PL, Cingulate cortex= CG, Accumbens Core =AcC, Accumbens Shell= AcSh, Dentate Gyrus= DG, Anterodorsal Thalamus= AD, Anteroventral thalamus= AV, Anteromedial Thalamus= AM, Perirhinal cortex= PRh, Entorhinal cortex= ENT, Granular Retrosplenial cortex= RSG, Agranular retrosplenial cortex= RSA, Supramammilar=SuM, Mammilar lateral= LM, Medial Medial Mammillary= MMM, Medial lateral Mammillary= MML Ventral Tegmental Area= VTA.

2.9 Statistical Analysis

The data recorded were analyzed using the SigmaStat software version 3.2 (Systat, Richmond, USA). In all cases, significance was accepted when $p < 0.050$. Mauchly's test was used to test the sphericity assumption in repeated-measures analysis. As the data met the sphericity assumption, uncorrected F tests were presented.

2.9.1 Behavioral data

The time spent in each of the four quadrants during the probe test was analyzed separately for each group and day, using a one-way ANOVA design (factor: quadrants,

four levels). Post hoc multiple comparison analyses were carried out, when allowed, using Tukey's test. Moreover, a non-parametric Friedman Repeated-Measures Analysis of Variance on Ranks was conducted when normality or equal group variances failed. Latencies were compared in the same way, separately for each group and day. The velocity and distance travelled were analyzed using a one-way ANOVA. Post hoc multiple comparison analysis was carried out, when allowed, using Tukey's test.

2.9.2 *c-Fos*

Six subjects were analyzed per group. Cell counts from the six selected sections for a given brain region in each animal were averaged, and the mean was used for statistical analysis. One-way ANOVA was used to assess whether the number of c-Fos positive nuclei was different between groups. When the ANOVA detected significant differences, Tukey post hoc tests were used to clarify differences between individual groups.

2.9.3 *COx activity*

Group differences in COx activity measured in each brain region were evaluated by one-way ANOVAs. A Kruskal–Wallis one-way analysis of variance of Ranks (H) was performed when equal variance failed. Tukey's test was applied as a post-hoc test when ANOVA was used, and Dunn's method when Kruskal–Wallis was used.

2.9.4 *Correlations*

The analysis of interregional correlations was performed by calculating Pearson product-moment correlations. In order to avoid errors due to an excessive number of significant correlations in small sample sizes, we used a 'jackknife' procedure: based on the calculation of all possible pairwise correlations resulting from removing one

subject each time, and taking into consideration only those correlations that remain significant ($p < 0.05$) across all possible combinations.

3 Results

3.1 Morris Water Maze tasks

Analysis of the escape latencies showed a reduction in escape latencies compared to the first training day for all the groups. In the control group, there was a significant reduction in escape latencies from day one to day 4 of training ($F_{(4, 39)} = 5.062$, $p = 0.003$). In addition, fourth day latencies were shorter than second day latencies. In the MS10 group, there was a significant reduction in escape latencies from day one to days 3 and 4 of training ($F_{(5, 39)} = 8.825$, $p < 0.001$), and fourth day latencies were shorter than second day latencies. In the MS21 group ($F_{(4, 39)} = 4.283$, $p = 0.008$), post-hoc tests revealed a significant reduction in escape latencies from the third to fourth day of training, compared to the first day, as occurred in the MS10 group. Analysis of the escape latencies on the fifth day (Reversal training) showed a reduction in escape latencies, compared to the first training, for MS10 and MS21. In the control group, there were no significant differences between the mean latency on the fifth day and the mean latency on the rest of the days.

Analyses of the time spent in the target quadrant during the probe tests are consistent with the latency results and show that all the groups learned the task. The control group shows learning on the fourth day (Day 1: $F_{(3, 39)} = 0.702$, $p = 0.559$; Day 2: $F_{(3, 39)} = 5.111$, $p = 0.006$; Day 3: $F_{(3, 39)} = 5.527$, $p = 0.004$; Day 4: $F_{(3, 39)} = 9.883$, $p < 0.001$). Post hoc tests revealed significant differences between Quadrant D and the rest of the quadrants ($p < 0.005$) on the fourth day. On the second and third days, Quadrant D was significantly different from Quadrants A and C, but not from B. On the first day, no

quadrant was preferred. Control subjects showed that, on reversal learning, their percentage of permanence in the new quadrant was higher than that of the other subjects (Day 5: $F_{(3, 39)} = 5.546$, $p = 0.004$), which can be seen in Figure 4 (C). The MS10 group showed learning on the third day (Day 1: $F_{(3, 31)} = 0.636$, $p = 0.600$; Day 2: $F_{(3, 31)} = 1.804$, $p = 0.177$; Day 3: $F_{(3, 31)} = 14.215$, $p < 0.001$; Day 4: $F_{(3, 31)} = 22.031$, $p < 0.001$). Post hoc tests revealed significant differences between Quadrant D and the rest of the quadrants ($p < 0.005$) from the third day. On the first and second days, no differences were seen. This group did not show reversal learning because their time spent in the goal quadrant was not long enough to reach the criteria. The percentage spent in C was higher than in the A and B quadrants, but not more than D, the previous goal (Day 5: $F_{(3, 31)} = 7.488$, $p = 0.001$), as shown in Figure 4 (D). The MS21 group also showed learning on the third day (Day 1: $H_{(3)} = 2.510$, $p = 0.473$; Day 2: $F_{(3, 39)} = 2.154$, $p = 0.117$; Day 3: $F_{(3, 39)} = 8.050$, $p < 0.001$; Day 4: $F_{(3, 39)} = 8.784$, $p < 0.001$). Post hoc tests revealed significant differences between Quadrant D and the rest of the quadrants ($p < 0.005$) on the third and fourth days. On the first and second days, no differences were seen. This group did not show reversal learning because their time spent in the goal quadrant was not long enough to reach the criteria. The percentage spent in C was higher than in quadrant A, but also D (Day 5: $F_{(3, 39)} = 5.260$, $p = 0.005$), as Figure 4 shows (E).

Figure 4- Morris Water Maze Results

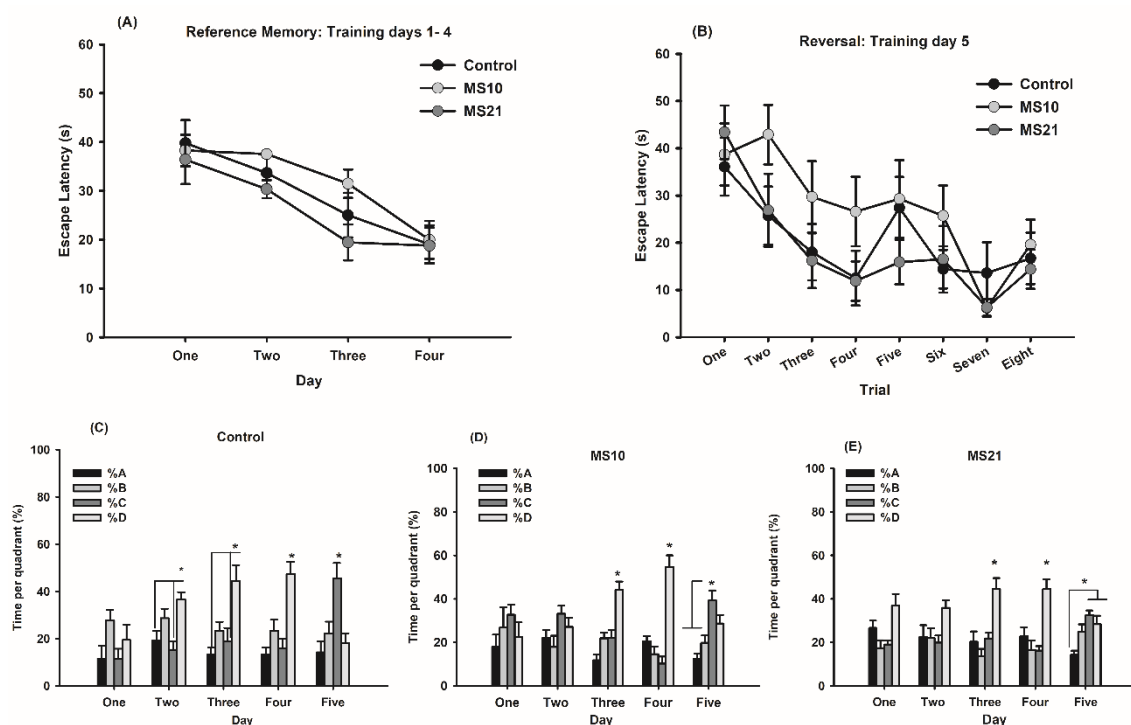


Figure 4 (A): Escape Latencies. The x-axis shows the days. All the groups showed longer latencies on the first day ($p < 0.005$). Maternal separation = MS (B): Escape latencies on each trial on day five (Reversal). (C) Permanence of control group in each quadrant (A, B, C, D). The x-axis shows the days. Control subjects reached the learning criteria on the fourth day ($p < 0.005$). They also learned the new location on day five (D) ($n=10$): Permanence of the MS10 group in each quadrant (A, B, C, D). The x-axis shows the days. MS10 subjects reached the learning criteria on day three ($p < 0.005$) ($n=10$). They did not reach the learning criteria on day five. (E): Permanence of the MS21 group in each quadrant (A, B, C, D). The x-axis shows the days. MS21 subjects reached the learning criteria on day three ($p < 0.005$). They did not reach the learning criteria on day five ($n=10$).

3.2 c-Fos

c-Fos positive cells per area were measured and averaged per subject and group. The Control group showed more c-Fos positive cells in mPFC areas: IL: $F_{(2, 17)} = 7,485$, $p=0.006$; PL: $F_{(2, 17)} = 7,717$, $p<0.005$; CG: $F_{(2, 17)} = 11,178$, $p<0.001$. There were no differences between groups on the anterior thalamus: AV: $F_{(2, 17)} = 1,206$, $p= 0.327$; AM: $F_{(2, 17)} = 2,035$, $p=0.165$. In the HC, MS10 showed more c-Fos activity than controls in both subareas, and more activity than MS21 in CA1. CA1: $F_{(2, 17)} = 9,752$, $p=0.002$; DG: $F_{(2, 17)} = 5,059$, $p=0.021$.

Figure 5- c-Fos positive cells

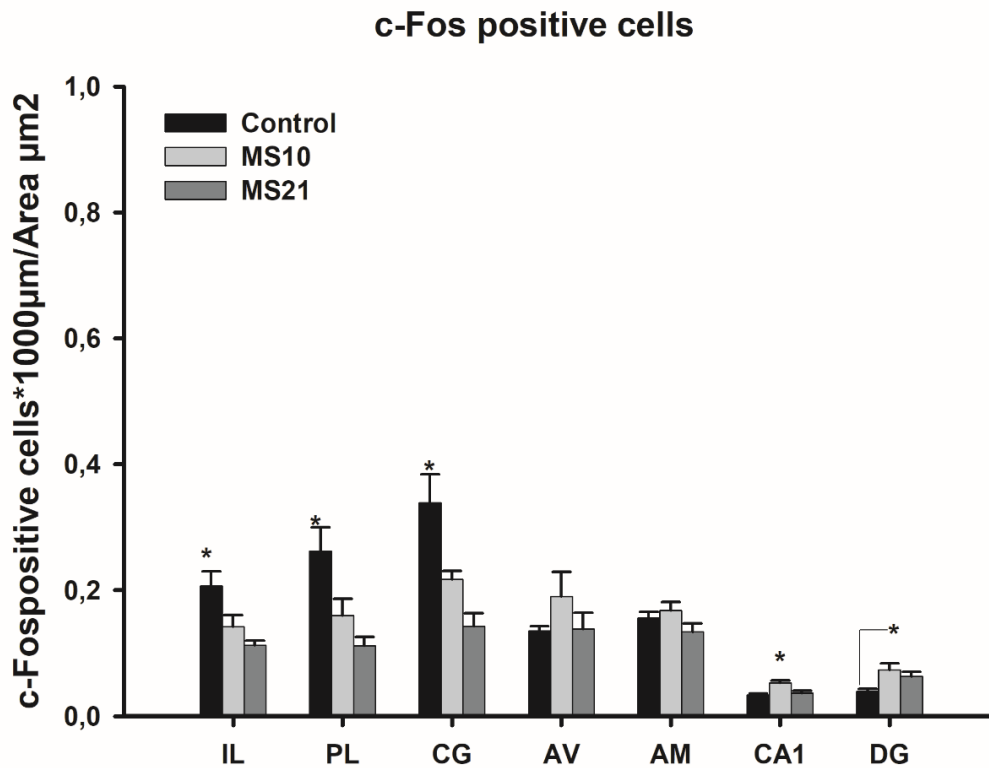


Figure 5: Figure 5 shows c-Fos positive cells per area. The number of c-Fos positive cells is greater in mPFC control groups ($p < 0.005$) ($n=6$). There are no differences in anterior thalamic nuclei. MS10 shows greater activity than controls in HC ($p=0.021$) ($n=6$), and more activity than MS21 in CA1 ($p=0.002$) ($n=6$).

3.3 COx activity:

COx activity analysis showed greater activity in MS10 than MS21 and controls in mPFC, dorsal and ventral striatum (core part of accumbens nucleus), hippocampus, thalamus (anterodorsal and anteromedial parts), and medial mammillary bodies: IL: $H_{(2)} = 10.829$, $p=0.004$; PL: $H_{(2)} = 12-120$, $p=0.002$; CG: $F_{(2, 22)} = 20.015$, $p < 0.001$; ST: $F_{(2, 22)} = 14.748$, $p < 0.001$; AcC: $F_{(2, 22)} = 9.462$, $p=0.001$; CA1: $H_{(2)} = 13.091$, $p=0.001$; CA3: $F_{(2, 22)} = 12.454$, $p < 0.001$; DG: $F_{(2, 22)} = 15.924$, $p=0.001$; AD: $H_{(2)} = 13.023$, $p=0.001$; AV: $F_{(2, 22)} = 17.554$, $p < 0.001$; MMM: $F_{(2, 22)} = 17.779$, $p < 0.001$; MML: $F_{(2, 22)} = 11.042$, $p < 0.001$. MS10 are more active than controls in the anteromedial thalamus,

perirhinal and entorhinal cortices, retrosplenial cortices, and supramamillar nucleus: AM: $H_{(2)} = 6.150$, $p=0.046$; PRh: $H_{(2)} = 9.531$, $p=0.009$; ENT: $F_{(2, 22)} = 0.765$, $p= 0.471$; RSG: $H_{(2)} = 17.919$, $p<0.001$; RSA: $H_{(2)} = 16.875$, $p<0.001$; SuM: $H_{(2)} = 14.829$, $p<0.001$. The MS10 group is also more active than MS21 in the Accumbens Shell: AcSh: $H_{(2)} = 6.582$, $p=0.037$. No differences were found in the lateral mammillary nucleus and ventral tegmental area: PIR: $H_{(2)} = 6.824$, $p=0.033$; MS: $H_{(2)} = 0.120$, $p=0.942$; BNST: $H_{(2)} = 5.959$, $p=0.051$; CeA: $H_{(2)} = 5.963$, $p=0.051$; BaA: $H_{(2)} = 4.182$, $p=0.124$; LM: $F_{(2, 22)} = 0.658$, $p= 0.529$; VTA: $F_{(2, 22)} = 2,855$, $p= 0.081$. In general, MS10 showed greater CO activity (Table 1).

Table 1- COx values

Structures	Control	MS10	MS21
IL	26,038 ± 3,464	39,696 ± 1,779**	28,379 ± 1,424
PL	29,62 ± 3,857	50,037 ± 2,889**	31,611 ± 1,206
CG	29,342 ± 3,478	55,794 ± 4,126**	30,371 ± 1,605
ST	26,657 ± 2,737	41,65 ± 1,658**	31,055 ± 0,86
AcC	29,077 ± 3,03	42,969 ± 2,078**	32,665 ± 1,24
AcSh	39,252 ± 3,907	53,104 ± 2,961 [#]	41,764 ± 1,155
CA1	19,255 ± 1,738	32,446 ± 2,193**	23,092 ± 0,438
CA3	18,933 ± 1,89	31,846 ± 2,388**	23,341 ± 0,814
DG	36,734 ± 3,18	57,291 ± 3,205**	40,084 ± 1,03
AD	48,897 ± 3,636	70,902 ± 2,91**	52,212 ± 0,866
AV	34,984 ± 3,262	54,559 ± 2,019**	42,044 ± 0,806
AM	24,405 ± 2,251	34,857 ± 2,905*	29,454 ± 0,969
PRh	23,771 ± 2,274	34,56 ± 3,503*	27,642 ± 0,788
ENT	25,289 ± 2,001	37,112 ± 2,695*	29,983 ± 1,011
RSG	29,289 ± 2,24	56,763 ± 5,218*	39,388 ± 1,265
RSA	25,655 ± 2,298	55,83 ± 3,976*	33,64 ± 0,782
SuM	24,707 ± 1,742	37,352 ± 2,149*	30,051 ± 0,678
LM	26,076 ± 3,263	30,892 ± 3,453	28,887 ± 1,755
MMM	21,069 ± 1,374	34,536 ± 2,04**	25,877 ± 1,208
MML	21,157 ± 1,394	34,685 ± 2,792**	26,778 ± 1,569
VTA	18,48 ± 0,971	21,243 ± 2,162	23,942 ± 1,587

Table 1: Shows the COx values (mean +/- SEM) in control and MS groups for all structures studied. Infralimbic cortex= IL, Prelimbic cortex=PL, Cingulate cortex= CG, Accumbens Core =AcC, Accumbens Shell= AcSh, Dentate Gyrus= DG, Anterodorsal Thalamus= AD, Anteroventral thalamus= AV, Anteromedial Thalamus= AM, Perirhinal cortex= PRh, Entorhinal cortex= ENT, Granular Retrosplenial cortex= RSG, Agranular retrosplenial cortex= RSA, Supramamillar=SuM,

Mamilar lateral= LM, Medial Medial Mammillary= MMM, Medial lateral Mammillary= MML Ventral Tegmental Area= VTA. *($p < 0.005$). *Higher than control, [§]Higher than control and MS21, # Higher than MS21

3.4 Correlations

Interregional correlations of COx activity are presented in figure 6 for the control group, which showed a greater number of them; figure 7 represents MS10 and MS21, respectively. Complete correlation tables are added afterward as tables 2, 3, & 4.

Figure 6- Interregional Correlations of Control Group

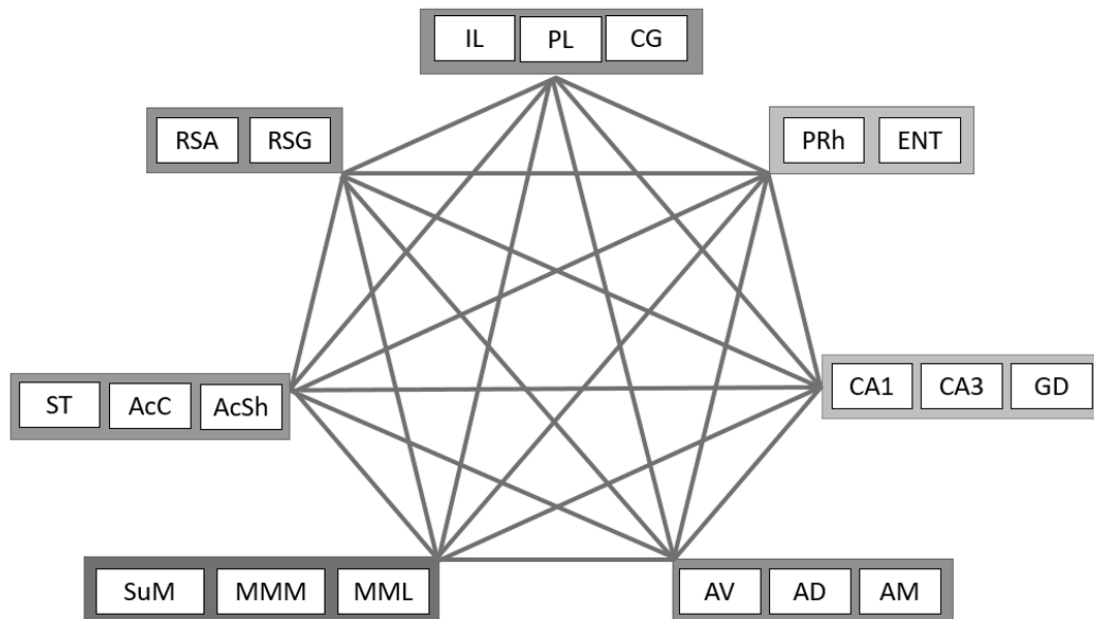


Figure 6: Shows schematic diagram of the significant interregional correlations of COx activity calculated for the different experimental groups. ($r < 0.7$, $P < 0.05$) ($n=10$ per group).

Figure 7- Interregional Correlations of Maternal Separation Groups

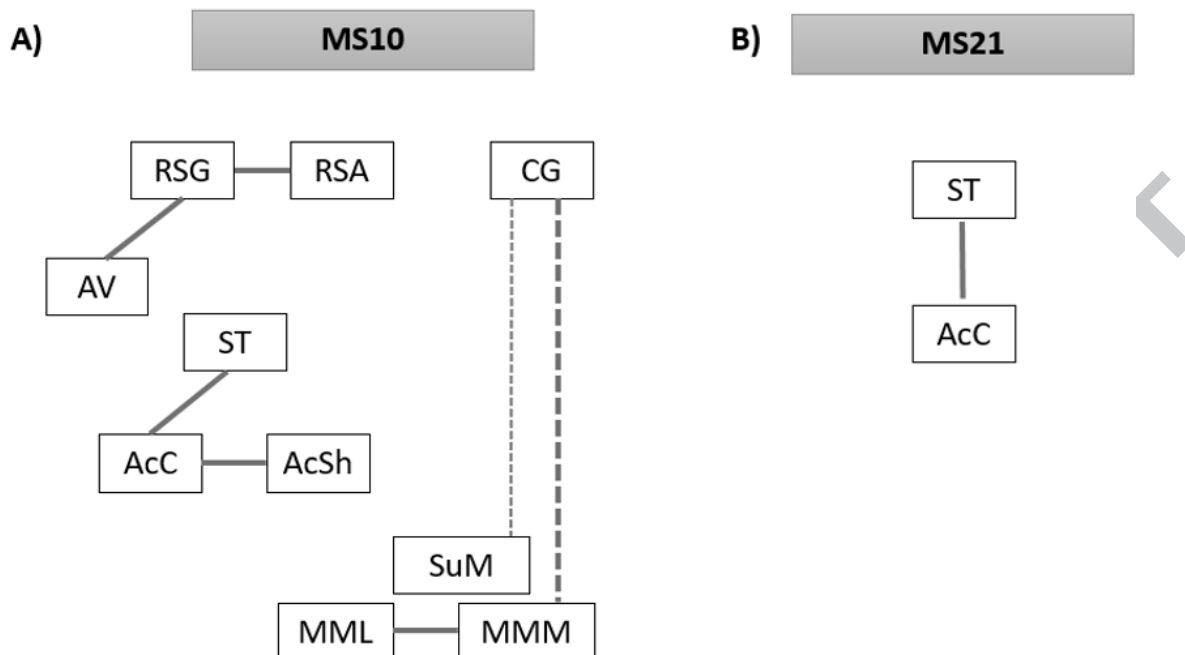


Figure 7: Shows a schematic diagram of the significant interregional correlations of COx activity calculated for the different experimental groups. A) MS10 group. B) MS21 group. Solid and dotted lines represent, respectively, highly positive and negative pair-wise Pearson's correlations ($r < 0.7$, $P < 0.05$) ($n=10$ per group).

CORRELATION TABLES

Table 2- Control Group Correlations

	CG	ST	AcC	AcSh	CA1	CA3
IL	0,98	0,83	0,80	0,76	0,93	0,88
	0,00	0,01	0,02	0,03	0,00	0,00
PL	0,99	0,84	0,82	0,78	0,94	0,88
	0,00	0,01	0,01	0,02	0,00	0,00
CG		0,89	0,85	0,82	0,96	0,91
		0,00	0,01	0,01	0,00	0,00
ST			0,96	0,98	0,93	0,83
			0,00	0,00	0,00	0,01
AcC				0,96	0,89	0,72
				0,00	0,00	0,04
AcSh					0,89	0,73
					0,00	0,04
CA1						0,90
						0,00
	AD	AV	AM	PRh	RSG	RSA
IL	0,62	0,86	0,92	0,77	0,91	0,85
	0,10	0,01	0,00	0,02	0,00	0,01
PL	0,64	0,88	0,93	0,80	0,91	0,87
	0,09	0,00	0,00	0,02	0,00	0,01

CG	0,72	0,92	0,91	0,84	0,94	0,92
	0,04	0,00	0,00	0,01	0,00	0,00
ST	0,89	0,99	0,91	0,92	0,96	0,85
	0,00	0,00	0,00	0,00	0,00	0,01
AcC	0,79	0,97	0,94	0,92	0,94	0,76
	0,02	0,00	0,00	0,00	0,00	0,03
AcSh	0,88	0,96	0,89	0,86	0,91	0,77
	0,00	0,00	0,00	0,01	0,00	0,03
CA1	0,81	0,94	0,92	0,84	0,91	0,89
	0,01	0,00	0,00	0,01	0,00	0,00
CA3	0,80	0,84	0,74	0,82	0,85	0,93
	0,02	0,01	0,04	0,01	0,01	0,00
DG	0,66	0,91	0,96	0,78	0,92	0,76
	0,08	0,00	0,00	0,02	0,00	0,03
AD		0,86	0,64	0,77	0,76	0,86
		0,01	0,09	0,03	0,03	0,01
AV			0,92	0,92	0,96	0,87
			0,00	0,00	0,00	0,00
AM				0,84	0,93	0,73
				0,01	0,00	0,04
PRh					0,93	0,78
					0,00	0,02
ENT					0,88	0,95
					0,00	0,00
RSG						0,84
						0,01

	SuM	MMM	MML
IL	0,52	0,83	0,86
	0,19	0,01	0,01
PL	0,56	0,84	0,87
	0,15	0,01	0,01
CG	0,58	0,87	0,90
	0,14	0,01	0,00
ST	0,69	0,94	0,93
	0,06	0,00	0,00
AcC	0,66	0,88	0,84
	0,07	0,00	0,01
AcSh	0,69	0,92	0,88
	0,06	0,00	0,00
CA1	0,71	0,93	0,95
	0,05	0,00	0,00
CA3	0,61	0,84	0,93
	0,11	0,01	0,00
DG	0,52	0,84	0,85
	0,19	0,01	0,01
AD	0,68	0,85	0,87

	0,07	0,01	0,01
AV	0,63	0,90	0,90
	0,09	0,00	0,00
AM	0,62	0,88	0,84
	0,10	0,00	0,01
PRh	0,70	0,86	0,86
	0,06	0,01	0,01
ENT	0,64	0,85	0,89
	0,09	0,01	0,00
RSG	0,57	0,89	0,89
	0,14	0,00	0,00
RSA	0,54	0,81	0,87
	0,17	0,02	0,01
SuM		0,85	0,80
		0,01	0,02
MMM			0,98
			0,00

Table 2: Shows the Pearson correlations between brain areas in the control group for all the structures studied.

Significant correlations after the jackknife procedure are in bold. Each table cell shows the calculated Pearson's correlation r value and the P level for the calculated correlation coefficient. Infralimbic cortex= IL, Prelimbic cortex=PL, Cingulate cortex= CG, Accumbens Core =AcC, Accumbens Shell= AcSh, Dentate Gyrus= DG, Anterodorsal Thalamus= AD, Anteroventral thalamus= AV, Anteromedial Thalamus= AM, Perirhinal cortex= PRh, Entorhinal cortex= ENT, Granular Retrosplenial cortex= RSG, Agranular retrosplenial cortex= RSA, Supramammilar=SuM, Mammilar lateral= LM, Medial Medial Mammillary= MMM, Medial lateral Mammillary= MML Ventral Tegmental Area= VTA. *($p < 0.005$).

Table 3- MS10 Group Correlations

	CG	ST	AcC	AcSh	CA1	CA3
IL	0,01	0,79	0,57	0,58	0,22	0,45
	0,99	0,03	0,18	0,17	0,64	0,31
PL	0,78	0,24	0,14	0,07	-0,63	-0,31
	0,04	0,61	0,77	0,87	0,13	0,50
CG		-0,29	-0,28	-0,35	-0,69	-0,67
		0,52	0,54	0,45	0,09	0,10
ST			0,92	0,85	0,16	0,43
			0,00	0,02	0,73	0,34
AcC				0,94	0,04	0,19
				0,00	0,94	0,68
AcSh					0,03	0,17
					0,95	0,72
CA1						0,85
						0,02
	AD	AV	AM	PRh	RSG	RSA

IL	0,04	-0,07	-0,05	-0,63	0,17	-0,05
	0,94	0,88	0,91	0,13	0,72	0,91
PL	0,57	0,42	-0,18	-0,19	0,55	0,69
	0,18	0,35	0,69	0,69	0,20	0,08
CG	0,53	0,56	-0,20	-0,07	0,63	0,87
	0,22	0,19	0,66	0,88	0,13	0,01
ST	0,02	-0,35	0,17	-0,66	-0,18	-0,37
	0,96	0,44	0,71	0,11	0,70	0,42
AcC	0,23	-0,22	0,49	-0,57	-0,09	-0,27
	0,61	0,63	0,27	0,19	0,86	0,56
AcSh	0,36	-0,15	0,57	-0,38	0,03	-0,21
	0,43	0,75	0,18	0,40	0,95	0,66
CA1	-0,75	-0,24	0,07	-0,24	-0,31	-0,66
	0,05	0,61	0,89	0,60	0,49	0,10
CA3	-0,66	-0,28	-0,07	-0,19	-0,33	-0,64
	0,11	0,55	0,89	0,68	0,47	0,12
DG	-0,43	-0,59	-0,08	0,34	-0,63	-0,74
	0,34	0,16	0,86	0,45	0,13	0,06
AD		0,60	0,50	0,25	0,72	0,77
		0,15	0,26	0,59	0,07	0,04
AV			0,47	0,33	0,94	0,84
			0,29	0,47	0,00	0,02
AM				0,10	0,44	0,16
				0,83	0,32	0,74
PRh					0,18	0,26
					0,71	0,57
ENT					0,09	0,27
					0,86	0,55
RSG						0,89
						0,01

	SuM	MMM	MML
IL	0,00	0,02	-0,07
	0,99	0,97	0,89
PL	-0,68	-0,70	-0,67
	0,09	0,08	0,10
CG	-0,87	-0,94	-0,79
	0,01	0,00	0,04
ST	0,48	0,38	0,15
	0,28	0,40	0,75
AcC	0,59	0,41	0,11
	0,17	0,37	0,81
AcSh	0,55	0,39	0,03
	0,20	0,39	0,94
CA1	0,55	0,73	0,85
	0,20	0,06	0,01
CA3	0,48	0,72	0,81

	0,28	0,07	0,03
DG	0,60	0,72	0,55
	0,16	0,07	0,20
AD	-0,37	-0,52	-0,70
	0,41	0,24	0,08
AV	-0,52	-0,43	-0,25
	0,23	0,34	0,59
AM	0,44	0,35	0,19
	0,33	0,45	0,68
PRh	-0,21	-0,05	-0,03
	0,66	0,92	0,95
ENT	-0,14	-0,10	-0,18
	0,77	0,83	0,70
RSG	-0,58	-0,54	-0,45
	0,17	0,21	0,31
RSA	-0,81	-0,83	-0,72
	0,03	0,02	0,07
SuM		0,93	0,73
		0,00	0,07
MMM			0,90
			0,01

Table 3: Shows the Pearson correlations between brain areas in the MS10 group for all the structures studied. Significant correlations after the jackknife procedure are in bold. Each table cell shows the calculated Pearson's correlation r value and the P level for the calculated correlation coefficient. Infralimbic cortex= IL, Prelimbic cortex=PL, Cingulate cortex= CG, Accumbens Core =AcC, Accumbens Shell= AcSh, Dentate Gyrus= DG, Anterodorsal Thalamus= AD, Anteroventral thalamus= AV, Anteromedial Thalamus= AM, Perirhinal cortex= PRh, Entorhinal cortex= ENT, Granular Retrosplenial cortex= RSG, Agranular retrosplenial cortex= RSA, Supramammilar=SuM, Mammilar lateral= LM, Medial Medial Mammillary= MMM, Medial lateral Mammillary= MML Ventral Tegmental Area= VTA. $*(p < 0.005)$.

Table 4- MS21 Group Correlations

	CG	ST	AcC	AcSh	CA1	CA3
IL	0,75	0,77	0,74	0,27	0,36	0,40
	0,03	0,03	0,04	0,51	0,38	0,33
PL	0,92	0,70	0,67	0,26	0,49	0,10
	0,00	0,05	0,07	0,53	0,22	0,82
CG		0,43	0,47	-0,06	0,73	0,11
		0,29	0,24	0,89	0,04	0,80
ST			0,85	0,72	-0,10	0,38
			0,01	0,04	0,82	0,36
AcC				0,51	0,01	0,52
				0,19	0,99	0,19
AcSh					-0,67	-0,13

					0,07	0,76
CA1						0,23
						0,58
	AD	AV	AM	PRh	RSG	RSA
IL	0,10	0,18	-0,22	0,46	-0,13	-0,05
	0,82	0,67	0,60	0,25	0,76	0,91
PL	0,00	0,52	0,14	0,09	0,22	0,47
	0,99	0,19	0,75	0,83	0,60	0,24
CG	0,02	0,38	0,18	0,15	0,10	0,46
	0,96	0,36	0,67	0,72	0,82	0,25
ST	-0,18	0,45	-0,09	0,09	-0,08	0,01
	0,68	0,26	0,83	0,83	0,86	0,98
AcC	0,12	0,68	0,20	0,31	-0,18	0,26
	0,79	0,06	0,63	0,46	0,68	0,54
AcSh	-0,45	0,31	-0,18	-0,29	0,08	-0,07
	0,27	0,46	0,67	0,49	0,85	0,87
CA1	0,23	0,03	0,31	0,17	0,05	0,28
	0,59	0,94	0,45	0,69	0,91	0,50
CA3	0,11	0,24	0,18	0,43	-0,74	-0,18
	0,79	0,57	0,67	0,29	0,04	0,67
DG	0,21	0,08	0,09	0,22	-0,22	-0,26
	0,61	0,86	0,83	0,60	0,60	0,54
AD		-0,04	-0,11	0,76	0,26	0,14
		0,93	0,79	0,03	0,54	0,75
AV			0,66	-0,11	-0,06	0,81
			0,07	0,80	0,90	0,02
AM				-0,42	0,01	0,64
				0,30	0,99	0,09
PRh					-0,28	-0,14
					0,51	0,73
ENT					-0,13	0,01
					0,76	0,98
RSG						0,28
						0,50
	SuM	MMM	MML			
IL	-0,02	-0,18	0,07			
	0,97	0,67	0,88			
PL	0,17	-0,23	0,06			
	0,69	0,58	0,89			
CG	0,35	0,04	0,14			
	0,40	0,92	0,74			
ST	-0,17	-0,36	0,18			
	0,69	0,38	0,67			
AcC	-0,32	-0,47	0,02			
	0,45	0,24	0,97			
AcSh	-0,53	-0,47	-0,02			

	0,18	0,24	0,96
CA1	0,61	0,38	0,21
	0,11	0,35	0,63
CA3	0,20	0,26	0,52
	0,63	0,54	0,19
DG	0,19	0,02	0,30
	0,65	0,96	0,47
AD	-0,15	-0,52	-0,69
	0,72	0,19	0,06
AV	-0,01	-0,29	0,15
	0,97	0,49	0,73
AM	0,05	0,10	0,23
	0,90	0,82	0,59
PRh	-0,04	-0,24	-0,33
	0,93	0,56	0,43
ENT	0,22	0,11	-0,05
	0,60	0,79	0,90
RSG	-0,24	-0,57	-0,68
	0,56	0,14	0,07
RSA	0,19	-0,22	-0,09
	0,66	0,60	0,83
SuM		0,71	0,63
		0,05	0,09
MMM			0,81
			0,02

Table 4: Shows the Pearson correlations between brain areas in the MS21 group for all the structures studied.

Significant correlations after the jackknife procedure are in bold. Each table cell shows the calculated Pearson's

correlation r value and the P level for the calculated correlation coefficient. Infralimbic cortex= IL, Prelimbic cortex=PL,

Cingulate cortex= CG, Accumbens Core =AcC, Accumbens Shell= AcSh, Dentate Gyrus= DG, Anterodorsal Thalamus=

AD, Anteroventral thalamus= AV, Anteromedial Thalamus= AM, Perirhinal cortex= PRh, Entorhinal cortex= ENT,

Granular Retrosplenial cortex= RSG, Agranular retrosplenial cortex= RSA, Supramammilar=SuM, Mammilar lateral= LM,

Medial Medial Mammillary= MMM, Medial lateral Mammillary= MML Ventral Tegmental Area= VTA. $*(p < 0.005)$.

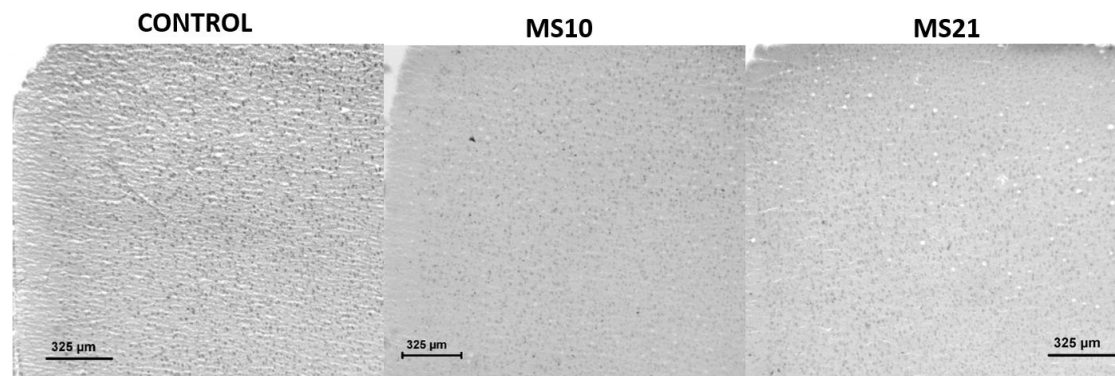


Figure 8: Figure 8 shows c-Fos positive cells staining on medial prefrontal areas (Cingulate cortex and prelimbic). Bars represent 325 µm. MS= Maternal separation.

4 Discussion

The analysis of the time spent in the target quadrant during the probe test shows that all the groups learned the reference memory task. These results agree with previous experiments (Sun et al., 2014). All the groups are aware of the task goal on days 3-4 of the training, which means that MS does not lead to alterations in spatial memory, at least not highly evident ones. This same behavioural result was also observed in males in our previous experiments (Banqueri et al., 2017; Lévy, Melo, Galef, Madden, & Fleming, 2003). The impairment produced by MS appeared when we asked the subjects to change their behavior. On reversal memory, we changed the invisible platform to another quadrant, opposite to the usual one. On this second task, separated animals were not able to complete the task successfully. They showed a lack of cognitive flexibility and tried to find the platform in its former location. They spent more time in quadrant D (previous) and less in quadrant C (new) than the control group. These results are consistent with previous research (Lomanowska & Melo, 2016). Interestingly, the MS10 group performed slightly better than the MS21 group, as seen in Figure 4 D (E). Despite not being statistically significant, MS10 started to show a preference for the quadrant of the new platform location, whereas MS21 did not show this preference. We tested this ability in adulthood. Some studies find no difference or even an increase in this flexibility in adolescence (Wang et al., 2015), whereas others

find the opposite, or worse flexibility, in adolescence (Thomas, Caporale, Wu, & Wilbrecht, 2016). Perhaps, the positive results are only present in adolescence, and our adulthood results are not comparable, or they may change in a sex-dependent fashion.

One of our limitations is the use of females and their subsequent hormonal variability. However, we can state that our females had regular cycles and were at different cycle points within the same cage. This variability allows us to imagine that our results were not due to sexual hormones, but more likely to the early-life stress.

Many groups use c-Fos as a brain activity marker (Kinnavane, Amin, Olarte-sánchez, & Aggleton, 2017; Soztutar, Colak, & Ulupinar, 2015). c-Fos-encoded protein, the product of the c-Fos oncogene, can in fact be used to measure brain activity, due to its expression indicating neuronal activity (Arias, Méndez, et al., 2015). We found a higher number of c-Fos positive cells in the mPFC of control females, who performed the task successfully. This increase in mPFC could be because reversal learning is PFC-dependent (Baudin et al., 2012). Some authors claim that impaired cognitive flexibility could be due to reduced functional connectivity in PFC (McEwen, Gray, & Nasca, 2015). mPFC is composed of IL, PL and CG cortices. Although all of them are related to spatial orientation and emotion, they display some specialized functional properties. First, CG is reciprocally connected with hippocampi and related cortices, whose connections are the key to activating representations during memory retrieval (Insel & Takehara-Nishiuchi, 2013). CG is also connected with the anterior thalamus. This link is used for both recollection and recognition memory (Aggleton, Dumont, & Warburton, 2011). The connection between CG and HC seems to be a controlling one because it has direct top-down control over HC memory processing (Eichenbaum, 2017). Therefore, CG activates and controls memory representations from the HC. Moreover, a lesioned CG impairs effort-based decision making (Powell et al., 2017), a classic prefrontal function. In the emotional field, CG has been related to anxiety (Felice et al.,

2014). MS produces changes in CG, and early-life stressed subjects show an increase in noradrenaline receptors in this area (Coccurello et al., 2014), possibly creating a sensitizing effect on the CG cortex when exposed to some stress molecules. MS also leads to a reduction in dopamine receptors in CG, and administration of D1 agonists improves memory deficits caused by this dopamine reduction (Lejeune et al., 2013). In addition, adverse experiences in early development seem to lead to neuronal loss in CG (Arborelius & Eklund, 2007) and reductions in soma size (Marković et al., 2014).

In addition, PL, like CG and IL, is also connected with the HC (Eichenbaum, 2017), and this cortex belongs to the cue–reward association network (Janak & Tye, 2015). The HC-PL connection is not only anatomical, but also functional. Theta oscillations with the entorhinal cortex (ENT) (a hippocampal related cortex) and PL are high when learning and consolidation are taking place (Insel & Takehara-Nishiuchi, 2013). Its specific functions inside the orientation brain network are associated with remote memory recall (Pereira de Vasconcelos & Cassel, 2015) and strategy shifting (Arias, Fidalgo, Vallejo, & Arias, 2014). PL adds the necessary cognitive flexibility to the spatial memory system (Aggleton et al., 2010) to change a non-successful behavior. Some authors claim that working memory deficits found in stressed animals are related to inflammatory processes in PL (Lukkes et al., 2017). In the emotional domain, as in CG, PL is also related to anxiety, and its malfunction is implicated in neuropsychiatric disorders (Chocyk et al., 2013). Stimulation of PL drives the inhibition of the stress axis (Sampedro-Piquero, Zancada-Menendez, Begega, Rubio, & Arias, 2013), and failure on the stress inhibition task may be the key to understanding its role in anxiety and associated disorders.

Finally, IL is involved in the formation of new choice patterns (Arias et al., 2014), not only in encoding spatial goals, but also in attentional processes and flexibility (Méndez-López, Méndez, López, & Arias, 2009). This function indicates that IL participates in discrimination learning (Fenton, Halliday, Mason, & Stevenson, 2014). When

glucocorticoid receptors are inhibited in IL but not in PL, stress sensitization and depressive-like behaviors arise (Poulos et al., 2014), showing the importance of IL in stress axis inhibition. When long-lasting MS occurs (later than PND 10), IL potentiation is impaired (Xiong, Yang, Wang, Xu, & Mao, 2014). All of these mPFC functions could be impaired, or at least reduced, in our MS groups, explaining the cognitive flexibility failure and the reduced c-Fos activity found.

These differences in c-Fos positive cells are diluted when we reach the anterior thalamus, where there were no differences between groups. In our opinion, the lack of significant results is also related to mPFC-increased activity in the control group. The mPFC areas lead the reversal training process and allow cognitive flexibility. In the hippocampi, we found more c-Fos positive cells in the MS10 group, which could indicate that this group is using the spatial memory system successfully. In the brain network, they show a mild impairment in mPFC that impedes finishing the task, but they try to compensate for this, with hippocampi bearing the costs. To sum up, mPFC seems to be the key to the failure in MS rats.

The landscape changes when we analyze the energy consumption in the same brains. First, MS10 shows more COx activity in all the studied areas. This means that even though they performed better than MS21 on the task, their energy metabolism cost is great. These results agree with previous findings from our laboratory, in which MS10 males who performed the reference memory task also showed high COx activity (Banqueri et al., 2017). Interestingly, these areas are the same for males and females, the hippocampal extended system network for spatial orientation. When we focus on the network used by each group, we notice that the control group is using all the measured areas together, with all the spatial memory areas previously described in the extended hippocampal system involved in the network (see Figure 5). However, the MS10 network is slightly less connected, and not all the areas work together (See Figure 6. A). The cingulate cortex shows an inverse correlation with mammillary nuclei,

(they have a tangible anatomic connection with the thalamus) (Jankowski et al., 2013), and the mild improvement in cognitive flexibility behavior could indicate the start of mPFC inhibition of a previous spatial learning occurrence, allowing new ones to take place. We also found two small networks: one inside the striatum (ventral and dorsal), which works with the hippocampus on spatial memory tasks and is related to the creation of new memories (Aggleton, 2012), and a second one with the anterior thalamus and retrosplenial cortex working together, probably showing the activation of the previous learning once it has been acquired.

On MS21 subjects, only two areas are related to their activity: ST and AcC (Figure 6. B). Striatal learning is associated with habits, which are inflexible by definition (Grissom et al., 2012). Therefore, if this group is expending their brain energy on habit-related areas, there is no place for prefrontal, cognitive flexibility. COx activity increases with sustained energy demands (Méndez-López, Méndez, López, Cimadevilla, & Arias, 2009), but greater energy demands sometimes result in less efficient work, as seen with the MS10 subjects. To sum up, a complex network of brain areas, as seen in the control group, is necessary to complete the tasks.

In conclusion, the use of two MS models allowed us to understand that differences in the separation protocols lead to different impairments. In this case, longer separations lead to a more intense impairment in cognitive flexibility. We found that brain activity is also altered. Regarding c-Fos activity, the control group showed more mPFC activity. If we further investigate the associated energy expenditure and the resulting network, we might obtain a broader perspective of the functional differences between healthy and stressed brains.

Further studies need to be carried out to discover why MS10 animals need more brain energy and what energy is expended for. Additionally, investigations will be necessary to explain whether mPFC impairment in MS animals is only functional or also structural. And most importantly, are these changes reversible? Once these questions are

answered, the development of therapeutic strategies to improve altered cognitive flexibility in early stressed subjects will be possible. Altered cognitive flexibility could be the key for learning and academic problems frequently found in early stressed human populations.

Acknowledgements

This research was supported by Project Grant of the MINECO (Ministerio de Economía y competitividad del Gobierno de España) PSI2017-83893-R, PSI 2015-73111-EXP, BES-2014-070562 to M.B.L., and Gobierno del Principado de Asturias, Consejería de Economía y Empleo, GRUPIN 14-088.

Conflicts of interest

None.

References

- Aggleton, J. P. (2012). Multiple anatomical systems embedded within the primate medial temporal lobe: Implications for hippocampal function. *Neuroscience and Biobehavioral Reviews*, 36(7), 1579–1596.
<http://doi.org/10.1016/j.neubiorev.2011.09.005>
- Arias, N., Fidalgo, C., Méndez, M., & Arias, J. L. (2015). How demanding is the brain on a reversal task under day and night conditions? *Neuroscience Letters*, 600, 153–157. <http://doi.org/10.1016/j.neulet.2015.06.014>
- Arias, N., Fidalgo, C., Vallejo, G., & Arias, J. L. (2014). Brain network function during shifts in learning strategies in portal hypertension animals. *Brain Research Bulletin*, 104, 52–59. <http://doi.org/10.1016/j.brainresbull.2014.04.004>
- Arias, N., Méndez, M., & Arias, J. L. (2015). Differential contribution of the hippocampus in two different demanding tasks at early stages of hepatic encephalopathy. *Neuroscience*, 284, 1–10.

<http://doi.org/10.1016/j.neuroscience.2014.08.060>

Banqueri, M., Méndez, M., & Arias, J. L. (2017). Spatial memory-related brain activity in normally reared and different maternal separation models in rats. *Physiology & Behavior*, *181*(May), 80–85. <http://doi.org/10.1016/j.physbeh.2017.09.007>

Barbosa Neto, J. B., Tiba, P. A., Faturi, C. B., De Castro-Neto, E. F., Da Graa Naffah-Mazacoratti, M., De Jesus Mari, J., ... Suchecki, D. (2012). Stress during development alters anxiety-like behavior and hippocampal neurotransmission in male and female rats. *Neuropharmacology*, *62*(1), 518–526. <http://doi.org/10.1016/j.neuropharm.2011.09.011>

Baudin, A., Blot, K., Verney, C., Estevez, L., Santamaria, J., Gressens, P., ... Naudon, L. (2012). Maternal deprivation induces deficits in temporal memory and cognitive flexibility and exaggerates synaptic plasticity in the rat medial prefrontal cortex. *Neurobiology of Learning and Memory*, *98*(3), 207–214. <http://doi.org/10.1016/j.nlm.2012.08.004>

Cabeza de Baca, T., & Ellis, B. J. (2017). Early stress , parental motivation , and reproductive decision-making : applications of life history theory to parental behavior. *Current Opinion in Pshychology*, *15*(Parenting), 1–6. <http://doi.org/10.1016/j.copsy.2017.02.005>

Coccorello, R., Bielawski, A., Zelek-Molik, A., Vetulani, J., Kowalska, M., D'Amato, F. R., & Nalepa, I. (2014). Brief maternal separation affects brain α 1-adrenoceptors and apoptotic signaling in adult mice. *Progress in Neuro-Psychopharmacology and Biological Psychiatry*, *48*, 161–169. <http://doi.org/10.1016/j.pnpbp.2013.10.004>

Dalaveri, F., Nakhaee, N., Esmailpour, K., Mahani, S. E., & Sheibani, V. (2017). Effects of maternal separation on nicotine-induced conditioned place preference and subsequent learning and memory in adolescent female rats. *Neuroscience*

Letters, 639, 151–156. <http://doi.org/10.1016/j.neulet.2016.11.059>

Dimatelis, J. J., Vermeulen, I. M., Bugarith, K., Stein, D. J., & Russell, V. A. (2016).

Female rats are resistant to developing the depressive phenotype induced by maternal separation stress. *Metabolic Brain Disease*, 109–119.

<http://doi.org/10.1007/s11011-015-9723-8>

Felice, V. D., Gibney, S. M., Gosselin, R. D., Dinan, T. G., O'Mahony, S. M., & Cryan, J. F. (2014). Differential activation of the prefrontal cortex and amygdala following psychological stress and colorectal distension in the maternally separated rat.

Neuroscience, 267, 252–262. <http://doi.org/10.1016/j.neuroscience.2014.01.064>

Neuroscience, 267, 252–262. <http://doi.org/10.1016/j.neuroscience.2014.01.064>

Gonzalez-Lima, F., & Cada, A. (1994). Cytochrome oxidase activity in the auditory system of the mouse: A qualitative and quantitative histochemical study.

Neuroscience, 63(2), 559–578. [http://doi.org/10.1016/0306-4522\(94\)90550-9](http://doi.org/10.1016/0306-4522(94)90550-9)

Grissom, E. M., Hawley, W. R., Bromley-Dulfano, S. S., Marino, S. E., Stathopoulos, N. G., & Dohanich, G. P. (2012). Learning strategy is influenced by trait anxiety and early rearing conditions in prepubertal male, but not prepubertal female rats.

Neurobiology of Learning and Memory, 98(2), 174–181.

Neurobiology of Learning and Memory, 98(2), 174–181.

<http://doi.org/10.1016/j.nlm.2012.06.001>

Insel, N., & Takehara-Nishiuchi, K. (2013). The cortical structure of consolidated memory: A hypothesis on the role of the cingulate-entorhinal cortical connection.

Neurobiology of Learning and Memory, 106, 343–350.

<http://doi.org/10.1016/j.nlm.2013.07.019>

Jankowski, M. M., Ronnqvist, K. C., Tsanov, M., Vann, S. D., Wright, N. F., Erichsen, J. T., ... O'Mara, S. M. (2013). The anterior thalamus provides a subcortical circuit supporting memory and spatial navigation. *Frontiers in Systems Neuroscience*,

Frontiers in Systems Neuroscience, 7(August), 45. <http://doi.org/10.3389/fnsys.2013.00045>

7(August), 45. <http://doi.org/10.3389/fnsys.2013.00045>

- Jenkins, T. A., Amin, E., Harold, G. T., Pearce, J. M., & Aggleton, J. P. (2003). Distinct patterns of hippocampal formation activity associated with different spatial tasks: A Fos imaging study in rats. *Experimental Brain Research*, 151(4), 514–523.
<http://doi.org/10.1007/s00221-003-1499-0>
- Kinnavane, L., Amin, E., Olarte-sánchez, C. M., & Aggleton, J. P. (2017). Medial temporal pathways for contextual learning : Network c- fos mapping in rats with or without perirhinal cortex lesions. *Brain and Neuroscience Advances*, 1–14.
<http://doi.org/10.1177/2398212817694167>
- Lejeune, S., Dourmap, N., Martres, M. P., Giros, B., Daugé, V., & Naudon, L. (2013). The dopamine D1 receptor agonist SKF 38393 improves temporal order memory performance in maternally deprived rats. *Neurobiology of Learning and Memory*, 106, 268–273. <http://doi.org/10.1016/j.nlm.2013.10.005>
- Loi, M., Mossink, J. C. L., Meerhoff, G. F., Den Blaauwen, J. L., Lucassen, P. J., & Joëls, M. (2015). Effects of early-life stress on cognitive function and hippocampal structure in female rodents. *Neuroscience*, (August).
<http://doi.org/10.1016/j.neuroscience.2015.08.024>
- Lomanowska, A. M., & Melo, A. I. (2016). Deconstructing the function of maternal stimulation in offspring development: Insights from the artificial rearing model in rats. *Hormones and Behavior*, 77, 224–236.
<http://doi.org/10.1016/j.yhbeh.2015.05.017>
- Lukkes, J. L., Meda, S., Thompson, B. S., Freund, N., & Andersen, S. L. (2017). Early life stress and later peer distress on depressive behavior in adolescent female rats: effects of a novel intervention on GABA and D2 receptors. *Behavioural Brain Research*, 330(January), 37–45. <http://doi.org/10.1016/j.bbr.2017.04.053>
- Majcher-maslanka, I., Solarz, A., Krzysztof, W., & Chocyk, A. (2017). The effects of early-life stress on dopamine system function in adolescent female rats.

International Journal of Developmental Neuroscience, 57, 24–33.

<http://doi.org/10.1016/j.ijdevneu.2017.01.001>

Marcondes, F. K., Binchi, F. J., & Tanno, A. P. (2002). Determination of the estrous cycle phases of rats: some helpful considerations. *Brazilian Journal of Biology*, 62(4a), 609–614. <http://doi.org/10.1590/S1519-69842002000400008>

Marković, B., Radonjić, N. V., Aksić, M., Filipović, B., Petronijević, N., Markovic, B., ... Petronijevic, N. (2014). Long-term effects of maternal deprivation on cholinergic system in rat brain. *BioMed Research International*, 2014. <http://doi.org/10.1155/2014/636574>

McEwen, B. S., Gray, J. D., & Nasca, C. (2015). Recognizing resilience: Learning from the effects of stress on the brain. *Neurobiology of Stress*, 1(1), 1–11. <http://doi.org/10.1016/j.ynstr.2014.09.001>

Méndez-López, M., Méndez, M., López, L., & Arias, J. L. (2009). Sexually dimorphic c-Fos expression following spatial working memory in young and adult rats. *Physiology & Behavior*, 98(3), 307–317. <http://doi.org/10.1016/j.physbeh.2009.06.006>

Méndez-López, M., Méndez, M., López, L., Cimadevilla, J. M., & Arias, J. L. (2009). Hippocampal heterogeneity in spatial memory revealed by cytochrome oxidase. *Neuroscience Letters*, 452(2), 162–166. <http://doi.org/10.1016/j.neulet.2009.01.056>

Paxinos, G., & Watson, C. (2005). *The rat brain in stereotaxic coordinates* (Fifth). Elsevier Academic Press.

Pereira de Vasconcelos, A., & Cassel, J. C. (2015). The nonspecific thalamus: A place in a wedding bed for making memories last? *Neuroscience and Biobehavioral Reviews*, 54, 175–196. <http://doi.org/10.1016/j.neubiorev.2014.10.021>

- Poremba, A., Jones, D., & Gonzalez-Lima, F. (1998). Classical conditioning modifies cytochrome oxidase activity in the auditory system. *European Journal of Neuroscience*, *10*(10), 3035–3043. <http://doi.org/10.1046/j.1460-9568.1998.00304.x>
- Soztutar, E., Colak, E., & Ulupinar, E. (2015). Gender- and anxiety level-dependent effects of perinatal stress exposure on medial prefrontal cortex. *Experimental Neurology*, *275*(June), 274–284. <http://doi.org/10.1016/j.expneurol.2015.06.005>
- Sun, X. M., Tu, W. Q., Shi, Y. W., Xue, L., & Zhao, H. (2014). Female-dependent impaired fear memory of adult rats induced by maternal separation, and screening of possible related genes in the hippocampal CA1. *Behavioural Brain Research*, *267*, 111–118. <http://doi.org/10.1016/j.bbr.2014.03.022>
- Thomas, A. W., Caporale, N., Wu, C., & Wilbrecht, L. (2016). Early maternal separation impacts cognitive flexibility at the age of first independence in mice. *Developmental Cognitive Neuroscience*, *18*, 49–56. <http://doi.org/10.1016/j.dcn.2015.09.005>
- Wang, Q., Li, M., Du, W., Shao, F., & Wang, W. (2015). The different effects of maternal separation on spatial learning and reversal learning in rats. *Behavioural Brain Research*, *280*, 16–23. <http://doi.org/10.1016/j.bbr.2014.11.040>
- Xiong, G. J., Yang, Y., Wang, L. P., Xu, L., & Mao, R. R. (2014). Maternal separation exaggerates spontaneous recovery of extinguished contextual fear in adult female rats. *Behavioural Brain Research*, *269*, 75–80. <http://doi.org/10.1016/j.bbr.2014.04.015>

Highlights

- Brain changes in two length models of maternal separation are compared in females.
- Spatial learning and flexibility are assessed in the Morris Water Maze.
- Maternally separated females show different degree of impairment in flexibility.
- Maternally separated females exhibit lower expression of c-Fos in prefrontal cortex.
- Maternal separation alters brain energy metabolic networks in the two models

ACCEPTED MANUSCRIPT